Available online at www.sciencedirect.com
SCIENCE DIRECT®
Journal of Hydrology 278 (2003) 51–63
Journal of Hydrology
www.elsevier.com/locate/jhydrol

New experimental techniques for pneumatic tomographical determination of the flow and transport parameters of highly fractured porous rock samples

C.I. McDermott[a,*], M. Sauter[b], R. Liedl[a]

[a]*Zentrum für Angewandte Geowissenschaften, University of Tübingen, Sigwartstr. 10, Tübingen D-72076, Germany*
[b]*Institut für Geowissenschaften, Georg-August University of Göttingen, Göttingen, Germany*

Received 4 July 2002; accepted 14 March 2003

Abstract

The investigation of flow and transport parameters in fractured porous material is difficult due to the high permeability contrast between the fracture networks and the porous material, and due to the question of the scale dependency of the parameters determined. Here experimental methods and new experimental equipment are presented using a pneumatic technique for the experimental tomographical investigation of highly fractured bench scale porous sandstone samples. The procedure allows a great deal of flexibility in the determination of the spatially variable flow and transport parameters and allows the question of scale to be addressed. Examples of the results gained from the application of these new techniques are given for both flow and transport parameter determination.

Keywords: Pneumatic tomography; Fractured rock; Experimental techniques; Flow and transport; Scale

1. Introduction

Recently the modelling and characterisation of flow and transport in fractured porous rocks have been receiving increasing interest in several geoscientific applications such as the consideration of water supply, contaminant transport, radioactive waste disposal, geothermal energy use and numerous geotechnical applications. Determination of the flow and transport parameters of the fractured porous system for predictive modelling is experimentally very difficult due to the large difference in the parameters for the fractures and the matrix of the rock, the complicated geometry of fracture networks and the scale of investigation which may be carried out. Usually one is either dealing with small laboratory samples containing one or two fractures, i.e. discrete investigation and discrete modelling, or with field scale tests where the processes known to be operating at a discrete scale combine to give an integral signal. This integral signal is very difficult to fully interpret in terms of the dominant processes, and exactly these processes are of great importance for the predictive modelling of flow and, in particular, transport in the system.

* Corresponding author. Fax: +49-7071-5059.
E-mail address: chris.mcdermott@uni-tuebingen.de (C.I. McDermott).

0022-1694/03/$ - see front matter © 2003 Elsevier Science B.V. All rights reserved.
doi:10.1016/S0022-1694(03)00132-X

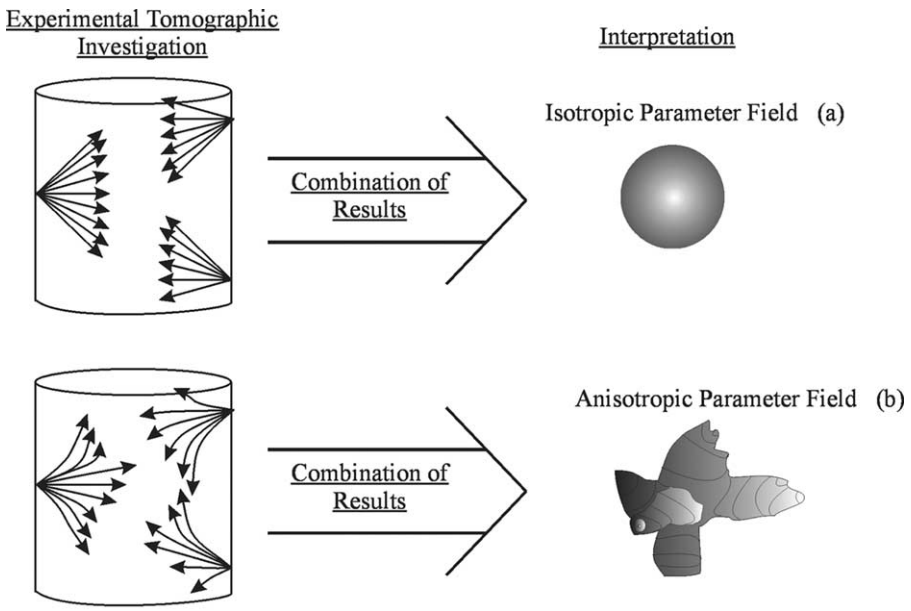

Fig. 1. Principles behind the tomographical investigation of a fractured sample with isotropic (a) and anisotropic (b) parameter distribution.

The concept of three dimensional tomographical investigation for the determination of the internal structure of a solid body based upon the distribution of measurable parameters is well established, and offers a method whereby more detail over the formation of the integral signal from several discrete elements can be derived. Techniques for applying this method to fractured rock are still under development. In principal the tomographic approach involves determining the parameter distribution within the body being investigated by combining several different spatially orientated measurements of particular phenomena. The combination and interpretation of these measurements allow a three dimensional image of the parameter distribution to be defined and thereby the structures causing this phenomena (Fig. 1). Examples can be found particularly in the field of medicine, e.g. Louis (1992). These principles can, however, also be applied to the investigation of the spatial distribution of parameters in rock or soil, e.g. Vesselinov et al. (2001a,b); Yeh et al. (2000); Gottlieb and Dieterich (1995); Lee and Uhlmann (1989); Jacquard and Jain (1965).

On a controlled laboratory scale there are a few examples of techniques used to interpret the three-dimensional flow and transport characteristics of fractured rock, particularly focusing on low porosity discretely fractured rock, for example, Vandergraaf et al. (1997). The question of up scaling of parameters has been addressed using laboratory techniques by a number of authors, including Tidwell and Wilson (1997); Niemi et al. (2000); McDermott (1999).

In this paper a flexible experimental technique is presented allowing the experimental tomographical investigation of large scale laboratory samples (30 cm diameter × circa 35 cm length). The samples contain fracture networks and the experimental procedure was designed to allow the measurement of discrete and integral signals for the constituent elements within the samples, i.e. matrix, individual fractures, fracture matrix interaction and fracture network response. The signals can be easily evaluated in terms of the geometry of the system and scale of measurement.

2. Application and method

In practical experimental terms to apply the tomographical investigation concept it is necessary

to make numerous point to point, or surface to surface measurements of flow and transport across a sample. Several point to point measurements are shown in Fig. 1(a) for a homogeneous isotropic sample and in Fig. 1(b) for an anisotropic sample. The results of the measurements are combined using an appropriate model to produce a parameter field representing the processes causing the signal measured. Here, we concentrate on the experimental procedure and apply a simplified model to present the types of results available from the equipment developed.

To allow the collection of such a large number of measurements, gas flow techniques were applied enabling rapid measurement of flow (pressure and flow rate) and transport (tracer concentration) signals. Using gas flow techniques means it is not necessary to saturate the samples prior to the investigation, and very small flow rates could easily be measured rapidly with a high degree of accuracy. In contrast, direct hydraulic tomographical investigation of such fractured porous samples has proved to be technically very difficult and time consuming (Hagemann, 2001) principally due to the problem of saturation. The saturation of the samples investigated was assumed to remain constant throughout the experimentation allowing the comparison of the results. The conversion of gas flow parameters to hydraulic parameters has been investigated in detail by Jaritz (1998) for one-dimensional flow systems. In the current experimental cell, flow is anisotropic and multidimensional. The detailed effects of slip flow (Klinkenberg, 1941) and free molecular flow (Carman, 1956) still need to be considered on hand of a modelled description of the flow system before a direct transfer of gas parameters to hydraulic parameters can be performed.

The difficulties and techniques for collecting fractured samples large enough so that the fracture network could be tomographically investigated but small enough still to be manageable in the laboratory is discussed in McDermott et al. (2003). Following the techniques presented in McDermott et al. (2003) the samples collected for the experimental work have a diameter of 30 cm and length of between 30 and 40 cm (Fig. 2). An example of the fracture record for such a sample is presented in Fig. 3.

In accordance with the concepts outlined above and the sample geometry, a special experimental cell was developed which allowed access to

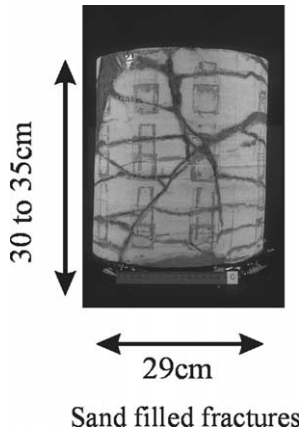

Fig. 2. Example of a fractured sample investigated with the techniques presented in this paper.

preselected positions along the surface of the sample (ports). Spatially orientated point to point measurements of the flow and transport characteristics could then be carried out from port to port. Additionally, the experimental cell was designed to adjust for samples differing in length (from 10 to 40 cm), diameter (290 mm ± circa 15 mm) and was able to maintain stable boundary conditions throughout the period of measurement. The principles and concepts behind the design of the cell to fulfil these criteria for reliable measurements of flow and transport measurements are presented in Fig. 4.

The experimental cell, named the multiple input output jacket (MIOJ), formed the key element in the experimental set up, the general arrangement of which is shown in Fig. 5. To investigate the flow and transport parameters a stable linear flow field is established across the sample from the input port/ports to the output port/ports. The flow rate across the sample is recorded using a flow meter (a bubble meter is illustrated). Gas tracer is then injected via a flow-through loop (Jaritz, 1998) in the flow field before the input port/ports and the breakthrough of the gas tracer at the output port/ports is recorded using a mass spectrometer. The exact mass of the tracer placed into the system is known, the location and the time of input, the mass recovered, location and rate of recovery is measured. Further details of the experimental procedure can be found in McDermott (1999).

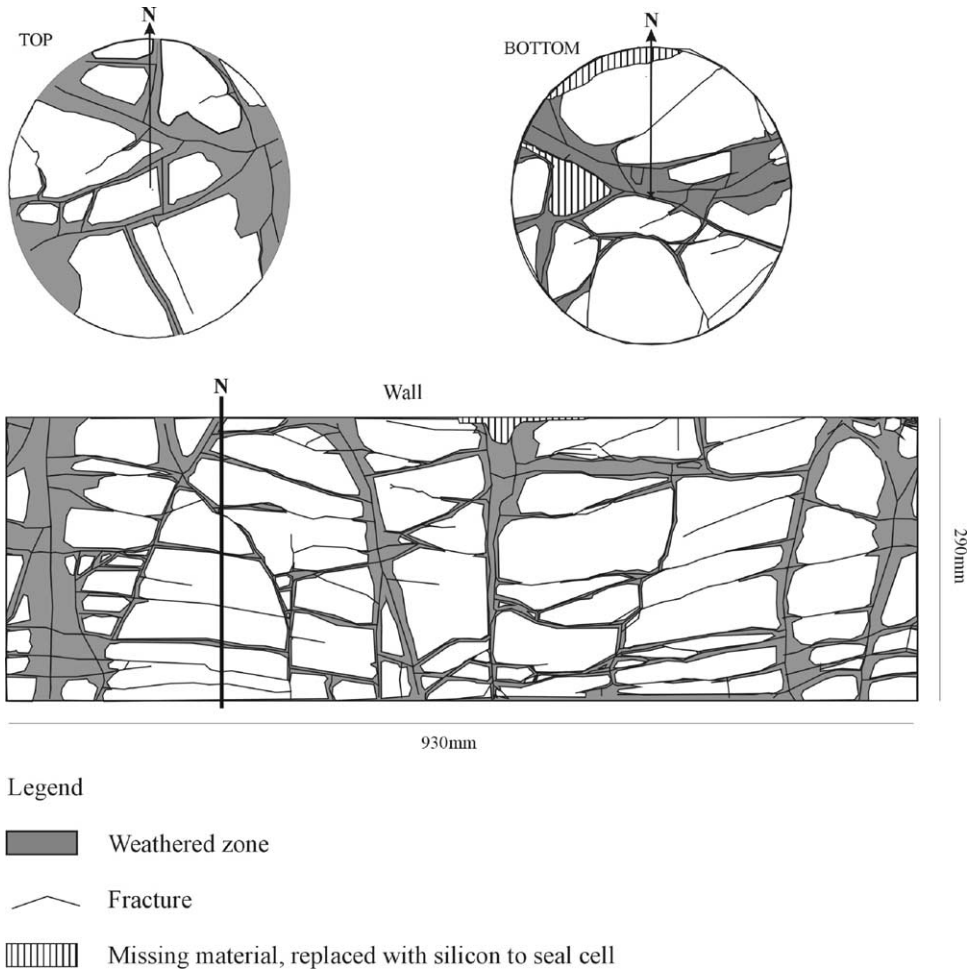

Fig. 3. Example of the nature of fracturing in a sample investigated, (height of sample 290 mm, diameter of sample 286 mm).

3. Technical details

The MIOJ, consists of two sealing membranes (outer and inner) with predefined open spaces or ports in them, three transparent curved polycarbonate shells (brace shells), two transparent polycarbonate circular plates (top/bottom plates) and a rigid frame. The functionality of the cell is achieved in that the membranes are pressed against the sample with the use of the brace shells and the top and bottom plate, thereby forming a complete cylinder hermetically sealing the sample, Fig. 6.

The outer sealing membrane is formed by a soft rubber seal 5 mm thick, the inner sealing membrane consists of a self adhesive elastomer 1–2 mm thick (Fig. 7), stuck to the outer sealing membrane. Under the influence of pressure from the supporting brace, the membrane deforms and adjusts to any unevenness along the surface profile of the sample thereby sealing any potential leaks. The ports for access to the sample are formed by the spaces in the membranes and each port can be connected to an external pressurised air supply through the connections in the supporting brace (Fig. 7).

As the individual brace shells are pressed onto the sealing membrane, the gap between the brace shells is filled with a soft rubber strip, of the same material as the outer sealing membrane. The thickness of these inter-brace shell sealing elements can be varied to account for variations in the diameters of the samples.

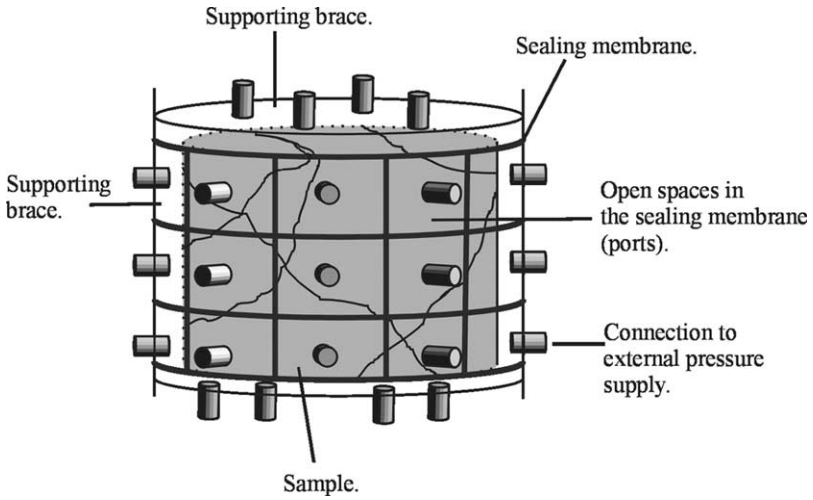

Fig. 4. Concepts and principles of the experimental cell enabling tomographic investigation of samples (sample diameter 30 cm, sample length up to 40 cm).

The supporting brace is held against the sample by four metal bands (Fig. 8). These bands are removable, and when screwed together exert an inwards radial force on the brace. The top and bottom braces are pressed against the sample from a rigid frame and a series of screws (Fig. 8).

4. Procedure

Hermetically sealing the sample in the MIOJ and ensuring that flow from port to port occurred through the sample and not along the surface of the sample as a result of the insufficient contact of the sealing membrane with the surface of the sample (Fig. 9) required a lot of care. The techniques employed during the construction of the MIOJ to ensure these conditions were achieved included

1. Ensuring that the sample was thoroughly cleaned from any fine loose material on the sample surface.
2. Any large scale unevenness or missing material from the sample was filled with silicon thus enabling the sealing membrane of the MIOJ to have a smooth contact with the surface of the sample.
3. Where the sample had a weak consistency a thin layer of silicon was placed around the locations of the input and output ports to aid in the sealing of these areas.
4. For highly fractured samples silicon was used to seal all the surface profile of the fractures apart from those areas appearing in ports. The silicon remained only on the surface of the sample and did not enter more than a couple of millimetres into the fracture itself consequently the permeability distribution remains practically unaffected. The silicon could be easily removed allowing re-measurement of the sample using a new geometrical set up of the ports.
5. The outer surface of the sealing membrane was lubricated to ensure an even distribution of the pressure applied by the supporting brace on the sample.

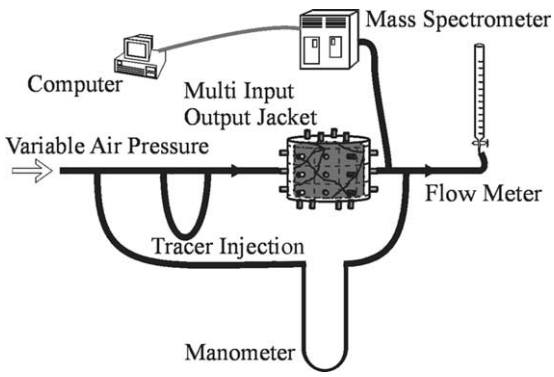

Fig. 5. Experimental set up.

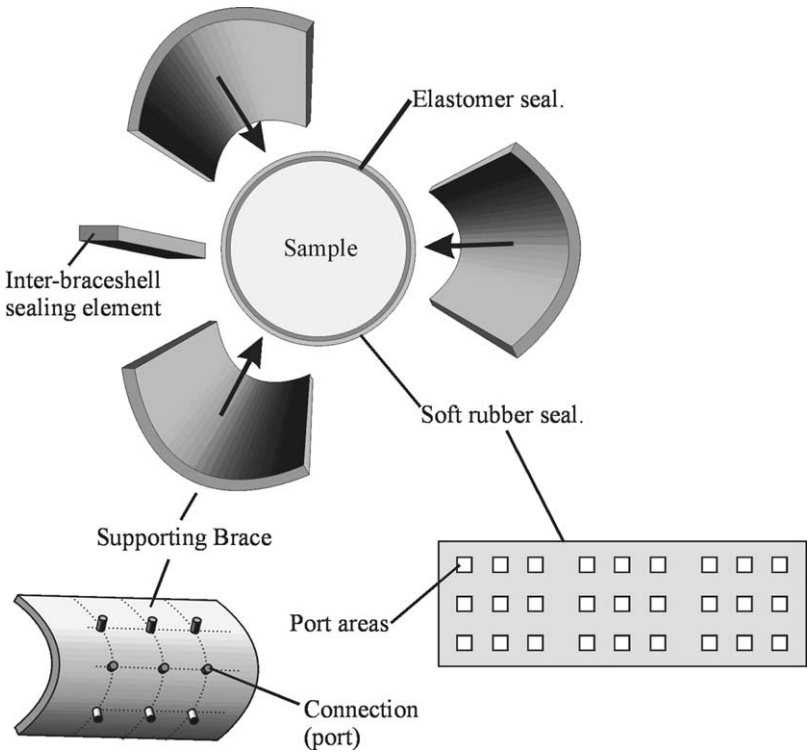

Fig. 6. Elements of the multiple input output jacket (MIOJ).

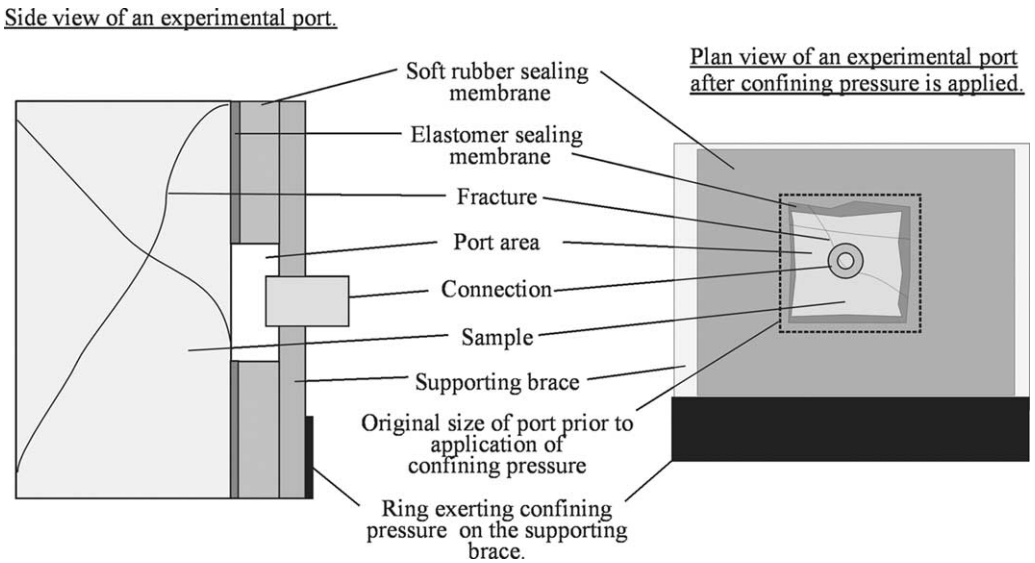

Fig. 7. Detailed view of technique used to isolate port areas on the surface of the sample.

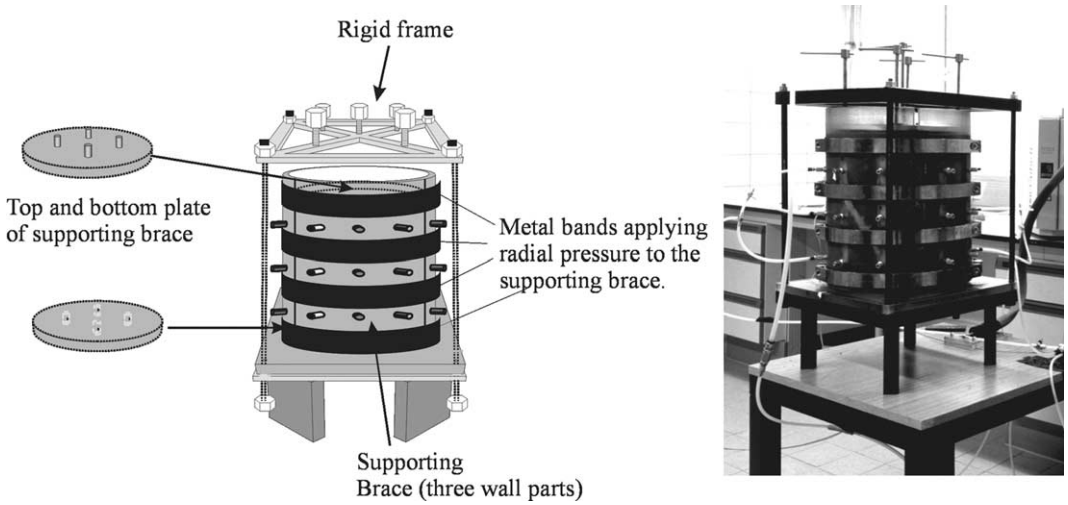

Fig. 8. Technical realisation of the principle behind the MIOJ.

Once the sample was sealed in the MIOJ, the apparatus was left for a period of 24 h to ensure the sealing elastomer (inner sealing membrane) had time to plastically deform and fill any unevenness in the sample profile or block any potential leaks in the system. After this period of time the air tightness of the MIOJ (comprising some 30 connections) was tested by ensuring it could maintain a pressure of some 150 mbar. Once it was clear that the system was air tight, stable benchmark flow measurements were made across the sample. After these results had been recorded, the pressure on the supporting brace (both edge and top and bottom) was increased slightly, the benchmark measurements repeated and the results compared. If the rate of flow remained constant then it was assumed that the flow was through the sample. However, if the flow rate had been reduced by an increase of pressure exerted by the supporting brace then flow along the surface of the sample and not through the sample was assumed to be occurring. In such cases the pressure exerted by the supporting brace was increased until no reduction in the flow rate was observed.

The benchmark measurements were repeated throughout the experimental investigation to ensure consistency of results. Both sealing membranes were deformable under light hand pressure, therefore, the effect of the pressure exerted by the supporting brace to ensure complete sealing of the sample on the fracture aperture due to the stiffness of the fractures was assumed to be negligible.

5. Flexibility of the MIOJ

Depending on the type of investigation required, different surface areas of the sample can be placed under a predefined pressure system thus allowing a variety of adjustable boundary conditions in an enclosed system. The flow direction across the sample can be easily varied, thereby the anisotropy of flow and transport parameters can be determined (Fig. 10). The MIOJ is not just limited to point to point

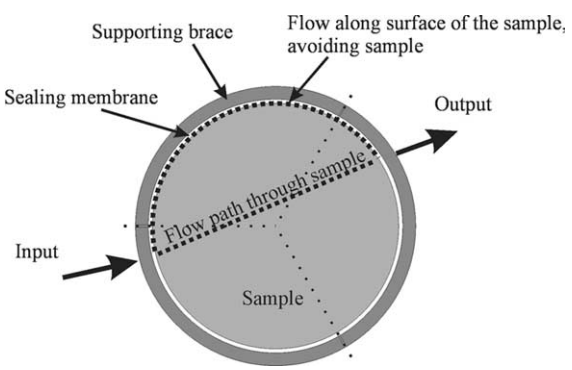

Fig. 9. Flow along the surface of the sample.

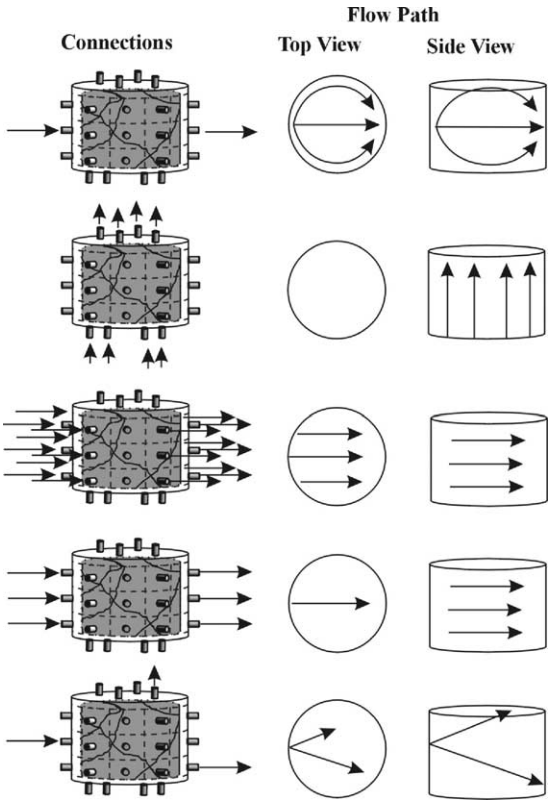

Fig. 10. Different input ports to output ports configurations, allowing the spatial investigation of the flow and transport characteristics.

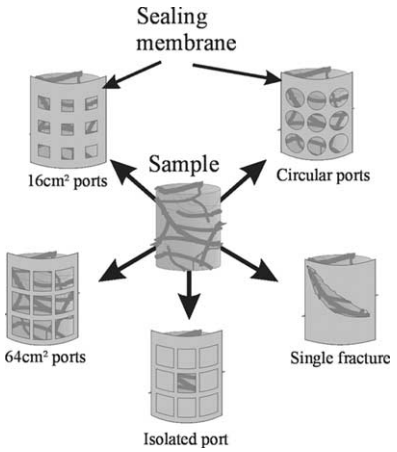

Fig. 11. Investigation possibilities of the MIOJ.

measurements, any combination of the ports can be used to measure the flow and transport parameters depending on the geometry of the sealing membrane (Fig. 11).

As can be seen from Figs. 10 and 11, dependency of the flow on scale effects such as the distance between the input and output ports or the size of the port area on the sample at a bench scale can be easily investigated as well as the effect of individual fractures in a fracture system or the fracture network itself.

6. Measurement of the flow field characteristics

The variable air pressure supply (Fig. 5), provided by a regulator valve, enabled a stable pressure difference to be established across the MIOJ. The flow rate across the sample as a result of this pressure difference was recorded using a flow meter. Experimental measurements indicated a linear relationship between flow and pressure difference with the application of a pressure difference of 150 mbar in the fractured system, allowing for the assumption that linear flow conditions were present within the samples.

In practise, it was assumed that the stable flow field was established by maintaining stable boundary conditions for a period of 5 min. For the samples investigated this period of time was determined experimentally by recording the change of the flow in the system against time from the initial conditions of 150 mbar plus atmospheric pressure in the whole sample, to the new boundary conditions, i.e. 150 mbar plus atmospheric pressure on the input port to atmospheric pressure on the output port. Fig. 12 records the change in flow rate with time for such an experimental set up for the cases where matrix is connected to the input port and in the steeper curve where a fracture is directly connected to the output port, for the gentler curve where matrix is connected to the output port. After 5 min relative stability in the flow measurements can be seen to have been achieved, however, true stability in the case of the matrix connection had only been achieved after 15 min.

Given the large number of measurements necessary to determine the spatially dependent flow and transport parameters, the time that would have been required to attain fully stable conditions, at least 15 min per point to point

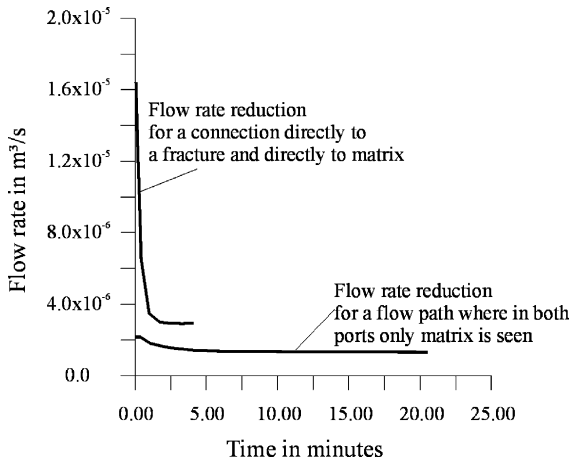

Fig. 12. Time taken for stabilisation of the flow field in the MIOJ samples, (example for sandstone samples with a matrix hydraulic conductivity of approximately 2.7×10^{-6} m/s where the entire sample was pre-pressurised to 150 mbar then flow allowed from the output port at 0 mbar).

experiment was not practically possible. For an investigation series comprising several hundred individual point to point experiments, the time required for the measurements would have increased by a factor of three, but the accuracy of the results minimally and, therefore, the error resulting from the possibility of slightly unstable flow conditions existing after 5 min was considered acceptable. Throughout an investigation series the cell was continually tested to prove that it was air tight, i.e. valves, the seals, the pipes and any connections were not leaking.

7. Measurement of the transport characteristics

To determine the transport characteristics of the system it was necessary to undertake tracer tests. Tracer gas (Helium) was injected into the system via a flow-through loop into the stable flow field once established across the MIOJ, (Fig. 5) to provide a Dirac pulse. The breakthrough of the tracer gas was recorded using a mass spectrometer.

This injection technique enables the exact mass of the tracer placed into the system and the time of input to be determined. If a constant pulse were used, the whole sample would become saturated with the tracer and prior to further experimentation the system would have to be flushed for a significant period of time.

To simplify the analysis of the transport information a non-reactive tracer gas, helium, was chosen as a tracer thus eliminating the possibilities of adsorption, retardation or biological degradation. In addition, the carrier gas used to establish the flow in the samples was air, and therefore, the selection of helium was particularly convenient in that practically no helium is found naturally in air.

8. Examples of data recorded

Applying the above procedure the following data is available after the completion of every individual experiment.

1. Rate of flow across the sample.
2. Area of input and output ports.
3. Pressure at input port and pressure at output port.
4. Orientation of the input port to output ports and, therefore, first estimation as to the geometry of the flow field.
5. Type and quantity of the tracer injected into the system.
6. The breakthrough curve of the tracer at every extraction point.

After several experiments the information available for each sample includes:

1. Different scaled spatially dependent information about the flow field parameters.
2. Different scaled spatially dependent information about the transport parameters.

9. Flow information

An extract example of the flow rate information recorded during experimentation is presented in Table 1. Examples of flow rate tensors derived from the experimental results for a highly fractured sandstone sample are presented in Figs. 13 and 14.

Table 1
Extract of data recorded in a pneumatic experimental investigation series

Input port number	Output port number	Pressure different (mbar)	Mass flow rate (m^3/s)	Direct distance between ports (m)	Port area (m^2)	Bearing deg. to north	Angle to horizontal
3	18	150	1.27E-05	0.285	0.001225	166.2	0.0
13	2	150	6.74E-06	0.296	0.001225	3.6	−19.7
15	2	150	5.39E-06	0.296	0.001225	3.6	19.7
5	16	150	2.03E-06	0.296	0.001225	148.8	19.7
1	14	150	4.29E-06	0.296	0.001225	183.6	−19.7
2	13	150	6.70E-06	0.296	0.001225	183.6	19.7
5	18	150	2.70E-06	0.296	0.001225	148.8	−19.7
3	14	150	4.96E-06	0.296	0.001225	183.6	19.7
1	32	150	8.04E-06	0.318	0.001225	186.8	−51.8
3	10	150	1.94E-05	0.318	0.001225	201.0	38.9
3	16	150	7.89E-06	0.348	0.001225	166.2	35.1
1	18	150	9.44E-06	0.348	0.001225	166.2	−35.1

In Fig. 13 three different levels of the sample are investigated via point to point measurements. In Fig. 14 the same sample is investigated along the length of the sides by connecting the input and output ports together.

From these simple diagrams the effects of scale on the measurement can immediately be seen. Using the more discrete point to point (Fig. 10) approach there is a variation of the flow rate dependent on whether a fracture is directly connected to the port used for

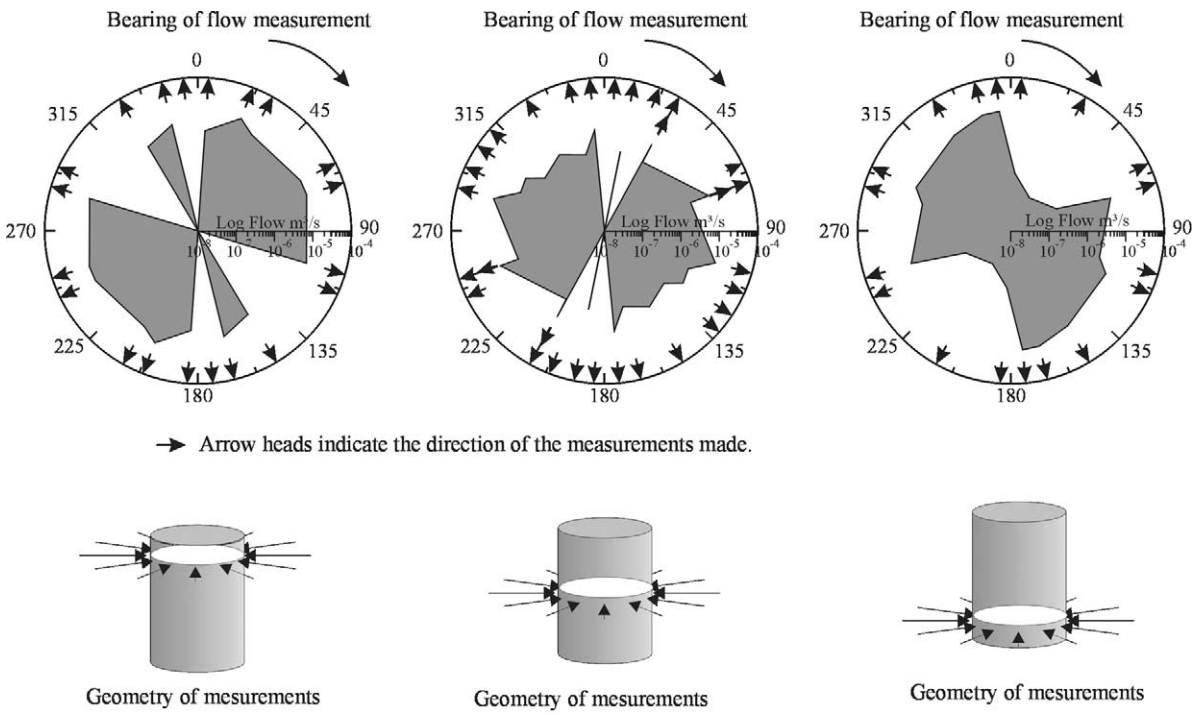

Fig. 13. Example of flow rate tensors derived from a highly fractured sample, here the tomographical investigation proceeds along three separate plains in the sample.

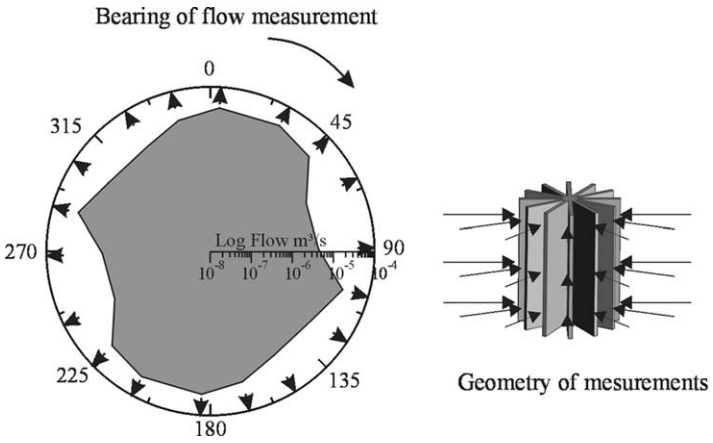

Fig. 14. Example of flow rate tensors derived from a highly fractured samples, here complete side-to-side measurements are made.

investigation. Some port to port flow rates are several orders of magnitude greater than others. However, using the more integral surface to surface approach an averaging effect occurs leading to the tensor seen in Fig. 14.

This effect of moving from the discrete investigation scale to a more integral investigation according to the size of the ports used for investigation is shown in Fig. 15. Here a simple one-dimensional Darcy model has been used to convert the flow data into apparent hydraulic conductivity to allow the comparison of different scales of measurement. The term apparent hydraulic conductivity refers to the fact that this Darcy model is a significant simplification of the complex system and provides an apparent hydraulic conductivity, however, the more accurate multiple dimensional analysis of the flow and transport signals to derive actual hydraulic conductivities, (e.g. Vesselinov, 2001a,b; Leven et al., 2000; McDermott et al., 1998) is beyond the scope of this current paper. In Fig. 15, it can be seen that the smaller investigation areas are, the larger the distribution in apparent hydraulic conductivity is. Likewise, the larger the areas are, the smaller the variation is. This illustrates the averaging effect of heterogeneities of a more integral signal in the larger areas, to the more discrete signals from the smaller areas.

10. Transport information

Typical results of transport experiments in the MIOJ are shown in Figs. 16 and 17. In Fig. 15 the characteristics are purely dominated by the matrix of the sample which lead to a signal with a comparatively long tailing and a large arrival time. In contrast, in Fig. 17 a number of different breakthrough curves are presented illustrating the variation in signal responses found from the MIOJ where a fracture was directly connected either to the input or output

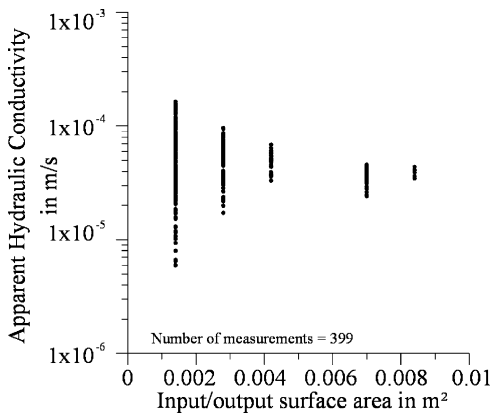

Fig. 15. Effect of the surface area on the variation in the apparent hydraulic conductivity.

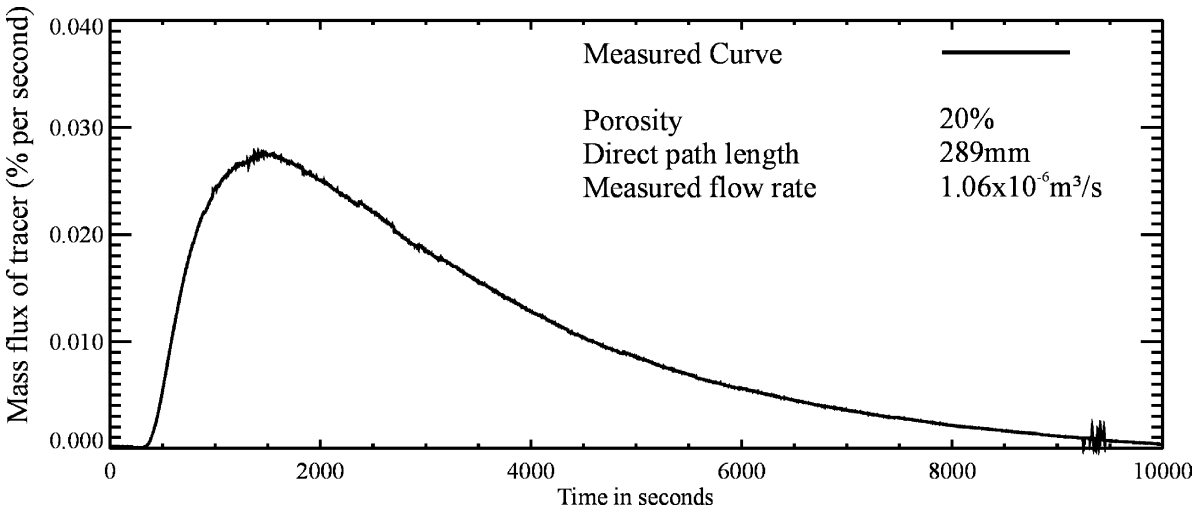

Fig. 16. Typical transport results from the MIOJ, dominated by matrix.

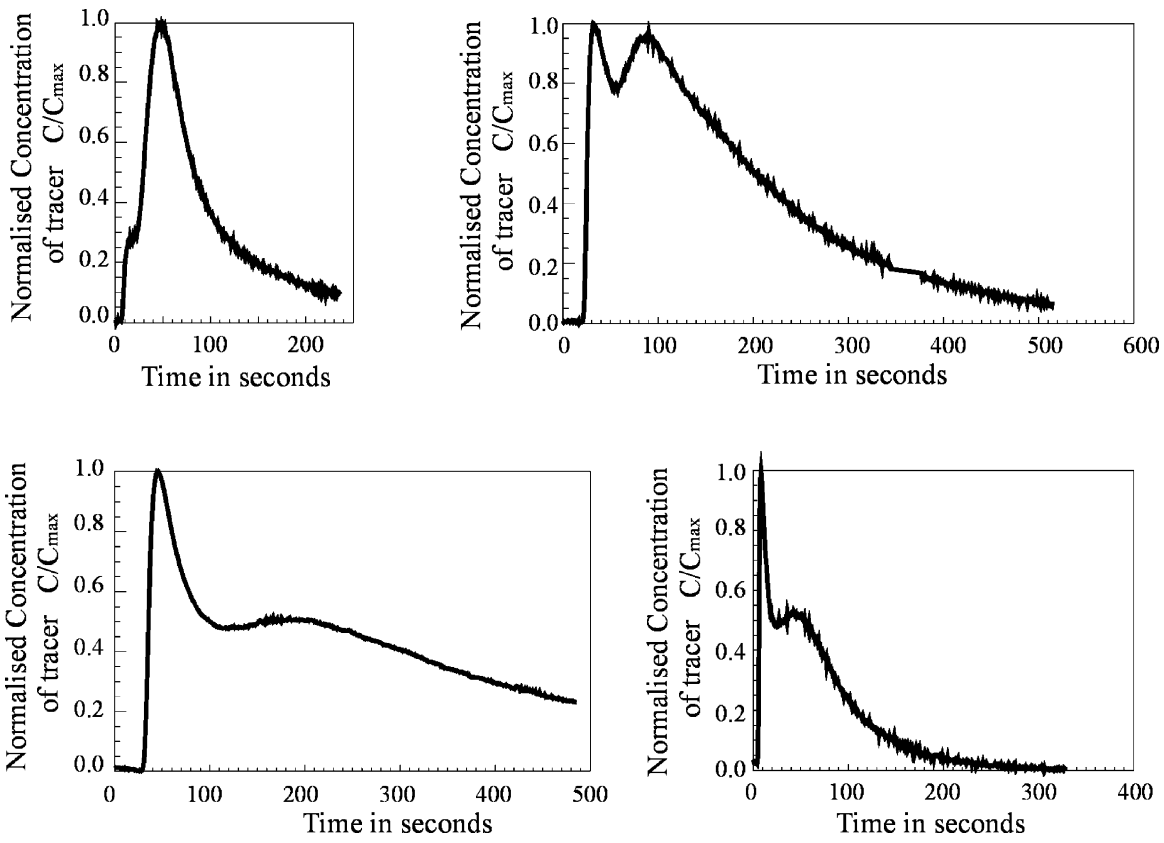

Fig. 17. Typical transport results from the MIOJ where fractures are directly connected to at least one of the investigation ports.

ports. Where fracture and matrix are involved in the transport then interesting double and even triple peaks have been observed. In addition the fracture network itself may also provide several different channels for flow leading to the derivation of different peaks for the arrival of the signal and several different ports may provide a signal from the fracture.

11. Conclusions

The MIOJ provides a flexible innovative approach for the experimental tomographical investigation of fractured porous rock. The experimental method developed provides a wide variety of options for investigating flow and transport in a fracture network. The results gained from experimentation to date show that it is possible to use the MIOJ to investigate fractured samples using a discrete and integral approach, to define orientated flow and transport tensors, and to investigate upscaling effects.

Acknowledgements

The authors wish to thank the German Research Foundation for the financing of this project.

References

Carman, P.C., 1956. Flow of Gases through Porous Media, Butterworths Scientific Publications, London.

Gottlieb, J., Dieterich, P., 1995. Identification of the permeability distribution in soil by hydraulic tomography. Inverse Problems 11, 353–360.

Hagemann, B., 2001. Untersuchung und Modellierung von Wasserdurchlässigkeit und Transporteigenschaften in geklüftetem Gestein, Diplomarbeit, Lehrstuhl für Angewandte Geologie, Universität Tübingen, Germany.

Jacquard, P., Jain, C., 1965. Permeability Distribution from Field Pressure Data, Institut Francais Du Petrole Rueil-Malmaison, France.

Jaritz, R., 1998. Quantifizierung der Heterogenität einer Sandsteinmatrix am Beispiel des Stubensandsteins. Dissertation an der Geowissenschaftliche Fakultät der Eberhard-Karls-Universität Tübingen. Germany

Klinkenberg, L.J., 1941. The permeability of porous media to liquids and gases. Drilling Production Practise, AM. Pet. Inst, Washington DC, pp. 200–213.

Lee, J.M., Uhlmann, G., 1989. Determining anisotropic real-analytic conductivities by boundary measurements. Communications on Pure and Applied Mathematics 42, 1097–1112.

Leven, C., McDermott, C.I., Baraka-Lokmane, S., Sauter, M., Liedl, R., Teutsch, G., 2000. 'Festgesteins-Aquiferanalog: Experimente und Modellierung—Laborexperimente und Entwicklung neuer Untersuchungsmethoden', 3. Workshop Kluftaquifere—Gekoppelte Prozesse, Institut für Strömungsmechanik im Internationalen Zentrum für Computergestützte Ingenieurwissenschaften (ICCES) der Universität Hannover.

Louis, A.K., 1992. Medical imaging: state of the art and future development. Inverse Problems 8, 709–738.

McDermott, C.I., 1999. New Experimental and Modelling Techniques to Investigate the Fractured Porous System. Dissertation an der Geowissenschaftlichen Fakultät der Universität Tübingen. Germany, pp. 170.

McDermott, C.I., Sauter, M., Liedl, R., 1998. Investigating Fractured-Porous Systems—The Aquifer Analogue Approach, Proceedings of the Third International Conference on Mechanics of Jointed and Faulted Rock, Vienna, pp. 607–612.

McDermott, C.I., Sinclair, B., Sauter, M., 2003. Recovery of undisturbed highly fractured bench scale samples (diameter 30 cm × 35 cm) for laboratory investigation. Engineering Geology vol. 69 (122), 161–170.

Niemi, A., Kontio, K., Kuusela-Lahtinen, A., Poteri, A., 2000. Hydraulic characterization and upscaling of fracture networks based on multiple-scale well test data. Water Resources Research 36 (12), 3481–3498.

Tidwell, V.C., Wilson, J.L., 1997. Laboratory method for investigating permeability upscaling. Water Resources Research 33 (7), 1607–1616.

Vandergraaf, T.T., Drew, J.D., Archambault, D., Ticknor, K.V., 1997. Transport of radionuclides in natural fractures: some aspects of laboratory migration experiments. Journal of Contaminant Hydrology 26 (vol. 1–4), 83–95.

Vesselinov, V.V., Neuman, S.P., Illman, W.A., 2001a. Three-dimensional numerical inversion of pneumatic cross hole tests in unsaturated fractured tuff: 1. Methodology and borehole effects. Water Resources Research 37 (12), 3001–3018.

Vesselinov, V.V., Neuman, S.P., Illman, W.A., 2001b. Three-dimensional numerical inversion of pneumatic cross hole tests in unsaturated fractured tuff: 2. Equivalent parameters, high-resolution stochastic imaging and scale effects. Water Resources Research 37 (12), 3019–3042.

Yeh, Jim, T.-C., Liu, Shuyun, 2000. Hydraulic tomography: development of a new aquifer test method. Water Resources Research 36 (8), 2095–2106.